

## DETECTION AND ANALYSIS OF HAZARDOUS LOCATIONS ON ROADS: A CASE STUDY OF THE CROATIAN MOTORWAY A1

Dražen Cvitanić, Biljana Vukoje

*Faculty of Civil Engineering, Architecture and Geodesy, University of Split, Croatia*

Submitted 24 June 2014; resubmitted 10 December 2014, 5 February 2015; accepted 8 March 2015;  
published online 31 January 2017

**Abstract.** The present paper describes research undertaken to identify causes underlying single-vehicle accidents (in terms of road design, driver behaviour and vehicle handling characteristics), which continuously happen in one specific section of Croatian motorway A1. The research resulted in a proposed procedure for a detection of hazardous locations on motorways and analysis of possible causes of single-vehicle accidents. The main part of the procedure involves test-rides with a vehicle equipped with devices (a ball bank indicator and a GPS data logger), which collect data on driver's behaviour and vehicle handling characteristics (position, speed, longitudinal and lateral acceleration, heading, path radius, etc.). Despite the fact that the motorway was designed in accordance with the design guidelines, test rides performed by higher operating speeds identified two locations with a lateral acceleration change a few times higher than the design value. The collected data are then used for analysing hypotheses about the possible causes of accidents by using a vehicle dynamic model. The hypothesis that a sudden change in lateral acceleration could result in a driver's inadequate manoeuvre like braking and cause a vehicle accident was analysed with a transient bicycle model. The results of test rides and the transient bicycle model indicate that speed, intensity of deceleration and underinflated tires significantly affect the probability of a single-vehicle accident.

**Keywords:** detection of hazardous locations; single-vehicle accidents; lateral acceleration change; ball bank indicator; GPS data logger; transient bicycle model; alignment inconsistency.

### Introduction

A large number of single-vehicle accidents happens on a few hundred meters long section of the motorway A1 Zagreb–Split (Fig. 1). Since the motorway completion in June 2004 until the end of 2012 there have been 22 single-vehicle accidents. The accidents resulted in 3 fatalities, 6 serious injuries and 12 minor injuries. There is no other section on motorway with recurring single-vehicle accidents.

According to the official reports all the accidents were caused by vehicle speeding. Most accidents happened between 4 p.m. and 8 p.m. in good weather and pavement surface conditions (dry pavement, no potholes, no mud, wetness or dirt, good visibility, no strong wind). A large number of single-vehicle accidents on some locations certainly points to the need for a detailed analysis of possible causes. Single vehicle accidents account for 10% of all accidents, but 45% of all accidents with fatalities (ERA-NET 2012).

Previous researches (Krammes *et al.* 1995; Hassan *et al.* 2001; Ng, Sayed 2004; Cafiso *et al.* 2004; Park, Sac-



Fig. 1. The accidents location and horizontal alignment of the analysed section

comanno 2006; Mattar-Habib *et al.* 2008; Cafiso, Cava 2009; Himes *et al.* 2011) have shown that one of the main reasons for accident occurrence is the geometric design inconsistency defined as the degree to which highway systems are designed to avoid critical driving manoeuvres and ensure safe traffic operation. A consistent road design ensures harmonized driving speed, in accordance with drivers' expectations and without sur-

prising events. The inconsistencies can cause situations in which drivers find themselves surprised by sudden changes in the alignment elements, which can lead to exceeding the limiting values of side friction or sudden change of lateral acceleration and loss of vehicle control.

The most frequently used and the most efficient design consistency criteria are based on operating speed. The speed consistency for a single road element can be assessed by comparing the operating and design speed while the evaluation of design consistency of successive elements can be performed based on the operating speeds of these elements (Lamm *et al.* 1995). The design consistency and safety in horizontal curves can also be evaluated by determining the margin of safety (the difference between side friction supply and side friction demand) (Lamm *et al.* 1995). Therefore, in the past sixty years many operating speed studies around the world have been conducted (TRB 2011).

In the phase of road design, an engineer can check the speed inconsistency between alignment elements by determining the speed profile from the operating speed model. Unfortunately, there are lot of combinations of the adjacent alignment elements, which could result in manoeuvres that are difficult to predict from speed profile in a road design phase. Some of them, such as sudden acceleration change, could lead to unexpected vehicle-driver behaviour and accident.

Therefore, the aim of this paper is to propose a method for a detection of alignment inconsistencies that cannot be observed with the standard consistency measures but may cause single-vehicle accidents. The proposed method is presented by the case study of the section of Croatian motorway A1 where accidents often occur. It consists of test drives with an equipped car with devices for measuring vehicle handling characteristics (speed, trajectory, lateral acceleration) making common manoeuvres with higher percentile operating speeds. Measured data are used to identify causes underlying single-vehicle accidents (in terms of road design, driver behaviour and vehicle handling characteristics). Single-vehicle accidents occur in curves usually due to loss of vehicle control (because of exceeded side friction supply or sudden change of lateral acceleration) or due to loss of vehicle stability (because of uneven deformation of front and rear tires).

The test rides identified locations with high values of lateral acceleration change (much higher than design values) exactly on section where accidents have occurred. In order to determine whether reaction on high lateral acceleration change can lead to vehicle accident, a vehicle dynamic model was used.

## 1. Road Alignment of Analysed Section

The A1 motorway design speed  $V_d$  is 130 km/h. According to Croatian Guidelines for Public Road Design (MPPV 2001) the minimum radius of horizontal curve (for  $V_d = 130$  km/h) is  $R_{min} = 850$  m applying the maximum superelevation  $e_{max} = 7\%$ . The minimum radius of crest vertical curve  $R_{min}^C$  is 27600 m, and the minimum radius of sag vertical curve  $R_{min}^S$  is 19000 m.

Test drives were performed on a 9 km long section of the motorway A1, from the intersection Vrpolje (334.5 km) to the service area Sitno (343.5 km), as shown on Fig. 1. Horizontal alignment of the selected road section consists of 6 reversed curves with geometric characteristics described in Table 1. It can be noticed that only transition between curves  $R_4$  and  $R_5$  is constructed without the use of spiral. The vertical alignment of the section consists of tangents with grades from 0.6% to 2% rounded with sag curve ( $R^S = 28000$  m).

Recorded accidents happened near km 340 on a transition between curves  $R_4$  and  $R_5$  i.e. at the flattest part of the analysed section with the elements that far exceed the minimum values (the horizontal and the vertical radius of the curve).

Table 1. Horizontal elements on the analysed section

|           | Element          | Radius [m] | Length [m] |
|-----------|------------------|------------|------------|
| $R_1$     | Horizontal curve | 1800       | 480        |
| $L_1$     | Spiral           |            | 200        |
| $L_2$     | Spiral           |            | 150        |
| $R_2$     | Horizontal curve | 1400       | 420        |
| $L_2$     | Spiral           |            | 150        |
| $L_3$     | Spiral           |            | 150        |
| $R_3$     | Horizontal curve | 1400       | 480        |
| $L_{3,4}$ | Spiral           |            | 150        |
| $R_4$     | Horizontal curve | 4800       | 2700       |
| $R_5$     | Horizontal curve | 4000       | 560        |
| $L_{5,6}$ | Spiral           |            | 200        |
| $R_6$     | Horizontal curve | 3500       | 2900       |

## 2. Field Research

Ten test rides were made on a 9 km long section with a test vehicle equipped with devices that record basic data about driver behaviour and vehicle handling characteristics. Data are collected in the wider area of the section where accidents happened in order to identify differences in vehicle-driver response between critical and surrounding sections, which could cause single-vehicle accident. The equipment used, data collection and the analysis procedure are described below.

### 2.1. Equipment Used

The test vehicle (*Peugeot 307*) was equipped with two devices: a ball bank indicator and a GPS data logger *PerformanceBox* (<http://www.vboxmotorsport.co.uk>). The ball bank indicator is an inclinometer (accelerometer) that is used by the US Federal and State Departments of Transportation for the purpose of determining safe curve speeds for horizontal curves (NHTSA 2001). It is a tube with a ball in a fluid. During the drive, the ball deviates from the neutral position due to superelevation, a body roll and side friction. It measures the side friction [in degrees], on a vehicle negotiating a horizontal curve.

One of the earliest ball-bank indicator studies was done by Moyer and Berry (1940). This study established

a relationship between the ball angle in degrees and the side friction factor. A recent research (Carlson 1995) recommended a slightly higher maximum side friction factors than Moyer and Berry. The relationship between the ball angle and the side friction factor according to Moyer, Berry (1940) and Carlson (1995) as well as the recommended speeds are presented in Table 2.

*PerformanceBox* is another device used in the test vehicle for gathering data about the vehicle handling characteristics. It is a 10 Hz GPS data logger based on the *Racelogic VBOX* (<http://www.vboxmotorsport.co.uk>), which is used by the car and tire manufactures to asses car and tire performance. *PerformanceBox* measures side friction, speed, braking distance, heading, path radius and more.

Table 2. Design side friction factors and ball bank angle

| Ball bank angle [°] | $f_{des}$          |                  | Recommended speed [mph] |
|---------------------|--------------------|------------------|-------------------------|
|                     | by Moyer and Berry | by Carlson model |                         |
| 14                  | 0.21               | 0.24             | ≤20                     |
| 12                  | 0.18               | 0.21             | 25–30                   |
| 10                  | 0.15               | 0.17             | ≥30                     |

### 2.2. Data Collection

The research was carried out with the test vehicle equipped with the listed devices. Ten test rides were made in each direction, from the intersection Vrpolje to the service area Sitno. The test drives were carried out in the coordination with the Croatian Motorways Ltd. – Hrvatske Autoceste (2015), a company for operation, construction and maintenance of motorways – during early morning hours when there is no intense traffic on the motorway. The data were collected under good weather and pavement conditions.

The speed limit on the highway is 130 km/h but the operating speeds are much higher. The operating speed is usually taken as 85th percentile of the speed distribution at a particular road section i.e. the speed below which 85th percentile of drivers actually drive. Average speed on Croatian motorways is 125 km/h with standard deviation of 15 km/h. The 85th percentile speed is 140 km/h, 95th percentile speed is 155 km/h and 99th percentile speed is 170 km/h. Since the vehicle, speeding was indicated as the cause of the accidents, it is suggested to make the test drives by experienced drivers (Jessen *et al.* 2001; Schurr *et al.* 2002). So, the test drives were performed with speeds in a range from 140–170 km/h.

Inclusion of operating speed in the design phase and the evaluation of the road alignment consistency is in the focus of many significant researches in recent years (Gibreel *et al.* 1999, 2001; Ottesen, Krammes 2000; Hassan 2004; Fitzpatrick *et al.* 2005; Marchionna, Perco 2008; Perco 2008; Medina, Tarko 2005; Cafiso, Cerni 2012; Wang *et al.* 2013).

*PerformanceBox* collected data on the test vehicle's speed, heading, path radius, longitudinal and lateral acceleration, time and position every 1/10 s. The ball

bank indicator data were video recorded with the time on the camera aligned with the time recorded with *PerformanceBox*. This allowed a precise determination of the locations where the ball bank indicator showed high values of deflection that can be uncomfortable for the driver (over 10°) when the driving speeds are high. According to the Table 2, these deflections correspond to the values of the side friction factor from 0.15 to 0.17. The ball bank indicator was used as a control device because of its mechanical nature (it gives not so detailed data as the GPS data logger, but it is reliable in every situation). *PerformanceBox* results with noise in data while the vehicle is in an underpass or in a tunnel, a frequent situation on motorways.

### 2.3. Presentation and Analysis of Recorded Data

The data recorded with *PerformanceBox* were processed and analysed using the software *PerformanceBox Tools*. Fig. 2 shows a part of the recorded data on the driving trajectory, turning radii, time elapsed, speed and lateral acceleration (expressed in 'g') for one test ride made with speed  $V \approx 165$  km/h.

The 'x' marker in the bottom right part of Fig. 2 represents the position of the measured data showed in the main data window under the graph. At this position, i.e. at the transition between the curves  $R_4$  and  $R_5$  in the direction from the East to the West (location 1 in Figs 1 and 2), *PerformanceBox* recorded a peak lateral acceleration of  $0.15 \text{ m/s}^2$ , while ball bank indicator recorded value of  $0.17 \text{ m/s}^2$ . The difference is probably due to fact that ball bank indicator records the impact of superelevation and body roll on a side friction value. It is important to note that both devices recorded peaks at the same locations.

The same peak value of lateral acceleration was recorded on the transition between curves  $R_4$  and  $R_5$  in the opposite direction, i.e. from the West to the East (location 2 in Figs 1 and 2). Locations 1 and 2 are both close to the connection point of curves  $R_4$  and  $R_5$ .

The recorded lateral acceleration values should not be critical for dry pavement with a high-quality surface. For dry pavement and worn tires, the slip coefficient of friction is rarely less than 0.5 (Sandberg, Ejsmont 2002). For wet pavement, depending on its macro texture, water depth, type and detritions of tires, the slip coefficient of friction falls below 0.2 for high-speeds (Clark 1971; Sandberg, Ejsmont 2002; Wong 2008).

According to these findings, it is almost unbelievable that the loss of vehicle control occurred just due to skidding. After all, the side friction factors from 0.12 to 0.18 have been recorded between reverse curves  $R_2$  and  $R_3$  and no accidents ever happened there.

Difference between these locations is in the change of lateral acceleration in time, i.e. the jerk [ $\text{m/s}^3$ ]. The recorded data shows that the maximum jerk on critical transition (between curves  $R_4$  and  $R_5$ ) is more than twice as high as in the transition between adjacent curves  $R_2$  and  $R_3$  with smaller radii. This sudden change of lateral acceleration on the transition between curves  $R_4$  and  $R_5$  is presented with a shaded area on the top of

the Fig. 2. The values of maximum jerk and minimum path radius determined from data collected for higher driving speeds on both driving directions are presented in Table 3.

While driving in the transition between curves  $R_5$  and  $R_4$  the lateral acceleration has been changed from 0 to 0.15-g ( $1.47 \text{ m/s}^2$ ) at an interval of 0.9 s. This resulted in a lateral acceleration change of  $1.6 \text{ m/s}^3$ , i.e. 6 times higher than the design value ( $0.25 \text{ m/s}^3$  for the speed of 130 km/h). At the critical transition, the test vehicle achieved a minimum path radius of 1420 m in location 1 (direction from East to West). The minimum recorded radius in location 2 (direction from West to East) was 1520 m and the lateral acceleration change was higher than  $1.10 \text{ m/s}^3$ . The ball bank indicator recorded almost the same values of jerk as *PerformanceBox* at both locations.

In each test drive, different trajectory and different values of the lateral acceleration were recorded, so the locations of the maximum acceleration and jerk differed, but no more than a few dozen meters. Each driver (or the same driver in different rides) differently perceives the location of transition between the curves and starts to steer a wheel in a different location, which results in different vehicle's trajectories i.e. minimum path radius. The differences in the vehicles trajectories explain the different values of the lateral acceleration at similar speeds, as well as the different location of achieving maximum lateral acceleration and jerk.

According to the findings stated above, there is an obvious inconsistency between the road alignment and driver's expectations, which resulted in extremely high values of lateral acceleration change. It is a pretty strange

Table 3. Recorded data on transitions between curves of analysed section

| $V = 155\text{--}170 \text{ km/h}$       | $R_{min} \text{ [m]}$ | Max jerk $[\text{m/s}^3]$ |
|--|-----------------------|---------------------------|
| <i>Direction from West to East</i>       |                       |                           |
| Transition $R_1 - R_2$                   | 1100                  | 0.25                      |
| Transition $R_2 - R_3$                   | 1120                  | 0.32                      |
| Transition $R_3 - R_4$                   | 3000                  | 0.28                      |
| <b>Transition <math>R_4 - R_5</math></b> | 1520                  | 1.10                      |
| Transition $R_5 - R_6$                   | 2400                  | 0.16                      |
| <i>Direction from East to West</i>       |                       |                           |
| Transition $R_6 - R_5$                   | 2600                  | 0.33                      |
| <b>Transition <math>R_5 - R_4</math></b> | 1420                  | 1.60                      |
| Transition $R_4 - R_3$                   | 1300                  | 0.45                      |
| Transition $R_3 - R_2$                   | 1240                  | 0.51                      |
| Transition $R_2 - R_1$                   | 1653                  | 0.65                      |

because this happens on a flattest part of analysed section, on a transition between curves with radii of 4800 m and 4000 m while it does not happen on the transitions between curves with smaller radii. The review of the road design showed that both curves on critical location have a crown cross slope, which means that the curve  $R_4$  has a negative superelevation in the East–West direction and the curve with  $R_5$  has a negative superelevation in the West–East direction. It was also found that the transition between the curves have been designed without the use of a spiral. All other transitions between curves on motorway are constructed with spirals and positive superelevation what explains the fact that there are no sudden changes in lateral acceleration.

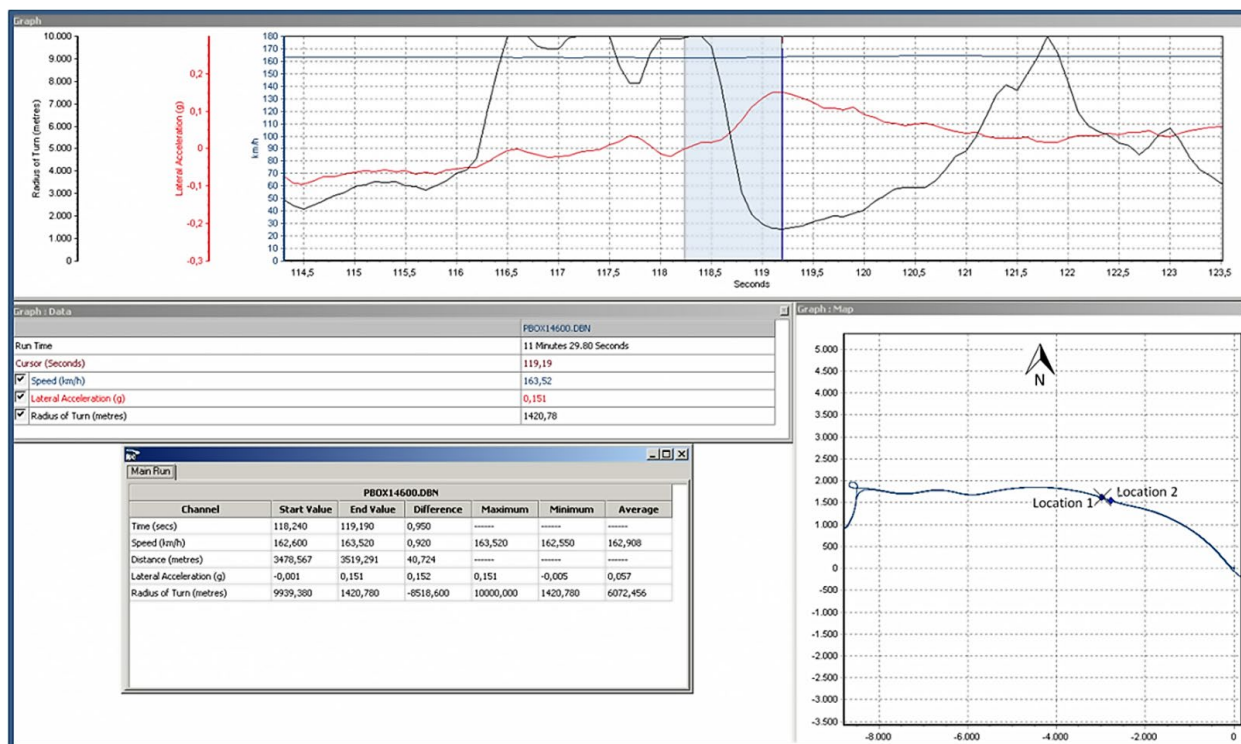


Fig. 2. Analysed data with *PerformanceBox Tools*

Both applied rules (no spiral and positive superelevation) on critical section are permitted for so high values of radii by the Croatian Guidelines for Public Road Design (MPPV 2001) and the majority of world road design guidelines. However, the high driving speeds encouraged with large curve radii in a combination with negative superelevation and absence of spirals between curves affected the test drivers' behaviour. In test rides, this combination resulted in trajectory with much smaller path radius than designed one and sudden jerk.

Therefore, there is a possibility that abrupt change in lateral acceleration surprised drivers who have reacted with inappropriate manoeuvre (like braking). Such inappropriate manoeuvre could lead to the loss of vehicle control or stability. The hypothesis stated above is further supported by the fact that there were no accidents since the end of the 2012 when speed limit around critical section was reduced to 120 km/h and media pointed to a large number of accidents in the section. In order to highlight the negative effect of high speeds, it is also important to note that in test rides with higher driving speeds, significantly lower path radii and higher jerks on critical transition between curves  $R_4$  and  $R_5$  were recorded. In test rides with speeds over 160 km/h, minimum path radius was always below 2000 m, while in test rides with speeds less than 150 km/h minimum radius was always over 2000 m.

In order to analyse the hypothesis that inappropriate manoeuvre like intense braking could lead to the loss of vehicle control, vehicle dynamic model (transient bicycle model) is used because it can describe the impact of superelevation, grade and speed changes on lateral acceleration and vehicle trajectory. Transient bicycle model was first used for calculation of lateral acceleration and vehicle path trajectory in order to replicate data from a test ride. After the model validation on test data, the scenario, which includes braking as a reaction on abrupt change in lateral acceleration was calculated. Based on calculated vehicle trajectory and lateral acceleration, conclusions about possibility of accident were drawn.

### 3. Vehicle Dynamic Models

All road design guidelines analyse vehicle motion in a curve as a point mass moving with a constant speed on a level terrain ignoring the impact of load distribution on front and rear tires caused by grade, acceleration, vehicle and tire characteristics. This simplified model is thus used as a basis for determination of the margin of safety in a process of design consistency evaluation for horizontal curves. However, the actual side friction demand on each tire (front or rear) can differ significantly from the value obtained with the point mass model. The greatest differences in calculated friction demands occur for decelerating vehicle on horizontal curve with downgrade i.e. the side friction demand on rear tires can be up to 30% greater than the friction obtained with the point mass model due to increased load on front tires. Additionally, simple point mass model considers only side friction demand caused by change of direction  $\frac{m \cdot V^2}{R}$  neglecting the part of side friction caused by the

tire deformation and its impact on vehicle trajectory and stability. It is therefore desirable to carry out detailed analysis of side friction, yaw motion and vehicle trajectory using the vehicle dynamic model. In the present paper, the bicycle model, which can describe basic terms of vehicle handling characteristics, is used for an analysis of the vehicle motion on one high-accident motorway section. The simplest bicycle model is the steady state model, which is concerned with the directional behaviour of a vehicle during a turn under non-time varying conditions. An example is a vehicle negotiating a curve with a constant radius at a constant forward speed. In order to describe the vehicle handling characteristics during the transition between the curves (changing the steering angle, superelevation and speed), in this study is used more complex model, i.e. transient bicycle model.

At low speeds, due to geometry of wheelbase the tires do not need to develop lateral forces because they just roll without slip angle (Wong 2008) so the average steering angle of the front wheels is equal to Ackerman angle (SAE International 2008; Nordeen, Cortese 1964)  $\delta = \frac{L}{R}$ , where  $L$  is distance between the front and rear axle;  $R$  is the curve radius. At high speeds, lateral acceleration is present in the curves and the tires must develop lateral forces so each tire has to deform, i.e., to develop an appropriate slip angle between the tire direction of heading and its direction of travel.

Fig. 3 shows the bicycle model where  $\alpha_f$  and  $\alpha_r$  are the slip angles of the front and rear tires, i.e., the angles between the longitudinal axis of the tires and the direction of travel caused by tire deformation, sideslip angle  $\beta$  is the angle between velocity vector  $V$  and the longitudinal axis of the vehicle at the centre of gravity;  $V_x$  and  $V_y$  are the components of velocity vector  $V$  in the longitudinal and lateral directions;  $\omega$  is the angular velocity;  $\delta$  is the front wheel steering angle;  $F_{xf}$  and  $F_{xr}$  are the tractive (braking) forces;  $F_{yf}$  and  $F_{yr}$  are the lateral tire forces;  $a$  and  $b$  are the distances from the front and the rear axles to the centre of gravitation.

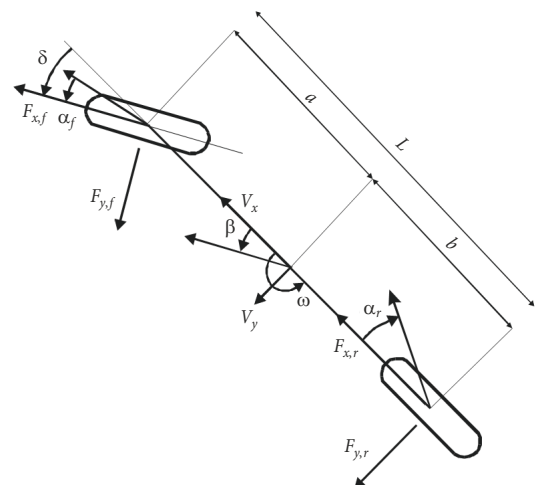


Fig. 3. Bicycle model

At high speeds, the steering angle needed for achieving a path radius depends not only on the distance from the front to the rear axle, but also on the slip angle at the front and the rear tires, approximately as follows (Bundorf 1967):

$$\delta = \frac{L}{R} + \alpha_f - \alpha_r. \quad (1)$$

The lateral force grows with the slip angle and at low slip angles this relationship is linear:

$$F_y = C_\alpha \cdot \alpha. \quad (2)$$

The proportionality constant cornering stiffness  $C_\alpha$  is defined as the slope of the curve at  $\alpha = 0$ . Cornering stiffness is dependent on many variables as tire size and type, number of plies, tire width and tread (Wong 2008). For a given tire, load and inflation pressure are main variables influencing cornering stiffness.

### 3.1. Cornering Equations

The transient vehicle model must be used in order to simulate the handling behaviour of the vehicle changing the speed and curvature. In the transient vehicle model, the inertia of the vehicle must be taken into consideration.

Referring to the Fig. 3, for a vehicle on a level road (no superelevation, no grade) the equations of motions with respect to the axes fixed to the vehicle body are given by (Wong 2008):

$$\begin{aligned} m \cdot \left( \frac{dV_x}{dt} - V_y \cdot \omega \right) &= F_{x,f} \cdot \cos \delta + F_{x,r} - F_{y,f} \cdot \sin \delta; \\ m \cdot \left( \frac{dV_y}{dt} + V_x \cdot \omega \right) &= F_{y,r} + F_{y,f} \cdot \cos \delta + F_{x,f} \cdot \sin \delta; \\ I_z \cdot \frac{d\omega}{dt} &= a \cdot F_{y,f} \cdot \cos \delta - b \cdot F_{y,r} + a \cdot F_{x,f} \cdot \sin \delta. \end{aligned} \quad (3)$$

In deriving the above equations, it is assumed that the vehicle body is symmetric about the longitudinal plane and the roll motion of the vehicle body is neglected. As one can see from Fig. 3 and Eq. (3), change in the steer direction results in tire deformation. Therefore, besides lateral acceleration component  $\frac{V^2}{R}$  caused by the direction change, lateral acceleration component  $\frac{dV_y}{dt}$  due to tire deformation with speed  $V_y$  appears.

The slip angles can be defined in terms of vehicle motion variables  $\omega$  and  $V_y$  using the small angle assumptions:

$$\begin{aligned} \alpha_f &= \delta - \frac{a \cdot \omega + V_y}{V_x}; \\ \alpha_r &= \frac{b \cdot \omega - V_y}{V_x}. \end{aligned} \quad (4)$$

For describing the vehicle handling behaviour on the recorded test vehicle trajectory, the transient bicycle model, which includes the impact of superelevation

$e$  [%], grade  $s$  [%] and vehicle deceleration  $a_{dec}$  [ $m/s^2$ ] was used. Combining Eqs (2)–(4) and assuming small angles, the equations of longitudinal, lateral and yaw motions of a vehicle with steering angle, superelevation and deceleration as input variables become:

$$\begin{aligned} \frac{dV_x}{dt} &= a_{dec} - \frac{C_{\alpha f}}{m} \cdot \left( \delta - \frac{a \cdot \omega + V_y}{V_x} \right) + V_y \cdot \omega + g \cdot s; \\ \frac{dV_y}{dt} &= \frac{C_{\alpha f} \cdot \left( \delta - \frac{a \cdot \omega + V_y}{V_x} \right) + C_{\alpha r} \cdot \left( \frac{b \cdot \omega - V_y}{V_x} \right)}{m} + \\ &\quad \frac{F_{x,f} \cdot \delta}{m} - V_x \cdot \omega + g \cdot e; \\ \frac{d\omega}{dt} &= \frac{a \cdot C_{\alpha f} \cdot \left( \delta - \frac{a \cdot \omega + V_y}{V_x} \right) - b \cdot C_{\alpha r} \cdot \left( \frac{b \cdot \omega - V_y}{V_x} \right) + a \cdot F_{x,f} \cdot \delta}{I_z}. \end{aligned} \quad (5)$$

In the above equations, steering angle  $\delta$  and braking (traction) force on front (driving) wheels  $F_{x,f}$  are time dependent. When the steering angle and external force are known, the response of the vehicle expressed in terms of the lateral acceleration, velocity and yaw velocity as functions of time can be determined by solving differential Eq. (5).

### 3.2. Calculation of Dynamic Equations of Vehicle Motion

The test vehicle was *Peugeot 307* and its characteristics (Baffet *et al.* 2009), i.e., model input data are presented in Table 4 (<http://www.cars-data.com/en/peugeot-307-2005/2003>). The tire and axle characteristics were obtained by using suspension characteristics and the *Dynatune* tire model (<http://www.dynatune-xl.com>). The tire and axle cornering stiffness presented in Table 4 are for the steady state vehicle behaviour on the level terrain. The front and rear tires cornering stiffness for the reference load are the same. However, as the cornering stiffness depends on the vertical load (Fig. 4), the front engine vehicle has a greater cornering stiffness on the front tires than on the rear.

There are multiple factors in vehicle design that influence the cornering characteristics of the axle besides the cornering stiffness of tires. The suspension and the steering system (roll moment distribution, camber change, aligning torque, etc.) are the primary sources of these influences (Wong 2008).

Thus, it can be seen that the rear axle cornering stiffness is greater than the front axle stiffness for the test vehicle although the rear tires stiffness is smaller than the front tires stiffness. It means that the slip angle of front tires is greater than that of the rear tires ( $\alpha_f > \alpha_r$ ) so the steering angle  $\delta$  required to negotiate a given curve increases with lateral acceleration. A vehicle with such handling characteristics is said to be understeer. When an understeer vehicle accelerates in constant radius curve, the driver has to increase steering angle  $\delta$ .

Table 4. Test vehicle characteristics

|                            |            |
|----------------------------|------------|
| Empty mass [kg]            | 1149       |
| Mass [kg]                  | 1447       |
| $L$ [m]                    | 2.60       |
| $a$ [m]                    | 1.12       |
| $b$ [m]                    | 1.48       |
| $I_z$ [kg·m <sup>2</sup> ] | 3000       |
| Front suspension           | McPherson  |
| Rear suspension            | Wishbone   |
| Tire                       | 195/65/R15 |
| $C_{af}$ tires [N/rad]     | 50000      |
| $C_{ar}$ tires [N/rad]     | 44000      |
| $C_{af}$ axle [N/rad]      | 70000      |
| $C_{ar}$ axle [N/rad]      | 93000      |

When driving, the stiffness of the tires and axles are constantly changing due to the load redistribution over the front and the rear axle caused by accelerating/decelerating or the grade, what is simulated by the transient vehicle dynamic model – Eq. (5). The transient bicycle model was calculated simulating a trajectory of the test vehicle driving from the East to the West in the critical section (Fig. 1). Three scenarios were simulated.

The scenario 1 tried to replicate the measured trials characteristics (speed, lateral acceleration, path radius) in order to validate the vehicle dynamic model.

The scenario 2 includes gently decelerating (2 m/s<sup>2</sup>) caused by a sudden change in lateral acceleration. The scenario 3 includes more intense decelerating (3.5 m/s<sup>2</sup>) and underinflated rear tires. All input data for scenarios 2 and 3 (vehicle and tires data, steering angles changes, speed) are the same as in the first scenario, except deceleration after the reaction on the beginning of jerk.

The simulation was performed for the transition from the curve  $R_5$  to  $R_4$ , in the East–West direction, with no spiral between curves and with a negative superelevation on the curve  $R_4$ .

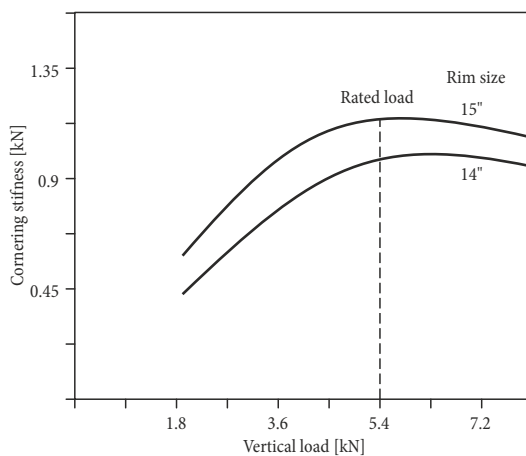


Fig. 4. Dependence of tire cornering stiffness on vertical load

The path curvature of the test vehicle varies in the transition between the two curves (Fig. 2). At the time  $t = 115$  s (when driving along the curve  $R_5$ ) the vehicle path radius is about 3000 m. Approaching to the curve  $R_4$  the vehicle drives almost straight for about 2 s and then, at the entering in the curve  $R_4$ , there is a sudden decrease in the path radius to the minimal value of 1420 m ( $t = 119.2$  s). After that point, the path radius increases (more than 9000 m at  $t = 121.8$  s) due to the change of the steering angle. After  $t = 122.5$  s, the path radius decreases to values under 5000 m, which corresponds to the designed radius.

The calculations were made for driving speed  $V = 175$  km/h, changing the value of steering angle according to recorded values in the test ride shown in Fig. 2. The simulation is started by driving straight from  $t = 0$  to  $t = 1$  s in order to set initial conditions ( $V_y = 0$ ,  $\omega = 0$ ,  $V_x = 48.6$  m/s), then continuing the test vehicle trajectory as described above. System of differential Eq. (5) has been solved by using the open source engineering software *Scilab* (<http://www.scilab.org>).

The simulation results for the test ride trajectory are presented in Fig. 5. In Fig. 5a it is seen that the maximum value of the lateral acceleration component due to the change of velocity direction  $\frac{V^2}{R}$  is about 1.7 m/s<sup>2</sup> (0.17g), corresponding to the radius of 1400 m, i.e., to the measured data. The maximum value of the lateral acceleration due to the change of velocity direction measured by the ball bank indicator was about 0.18g. Fig. 5b shows the values of lateral acceleration caused by tire deformation  $\frac{dV_y}{dt}$ . The direction of tire deformation reduces total lateral acceleration, as shown in Fig. 5c. Fig. 5d shows the path radius of the vehicle during the simulation, where it is possible to see how at first it changes from  $\infty$  to the minimal value of cca 1400 m. After that, it increases to more than 9000 m and then decreases and stabilizes to a value of about 4000 m, what is very close to actual data.

Therefore, the simulated trajectory and the vehicle handling characteristics data coincide very well with the actual data. It shows that the vehicle bicycle model can be used for modelling vehicle handling and transition behaviour.

After the validation of the bicycle model on actual data, the second scenario, which includes braking caused by a sudden change in lateral acceleration, was simulated. Deceleration of 2 m/s<sup>2</sup> was included after the reaction on the beginning of jerk. Due to decelerating, there is a load transfer to the front axle so the rear axle cornering stiffness decreases and the front axle stiffness increases according to Fig. 4.

One consequence of decelerating is a somewhat greater total lateral acceleration. There is a load distribution from the rear to the front tires due to braking, so the rear tires have to deform more to keep the required side friction force. As the rear slip angle increases, the vehicle path radius decreases for the same steering angle, i.e., the vehicle drifts slowly to the centre of the curve radius.

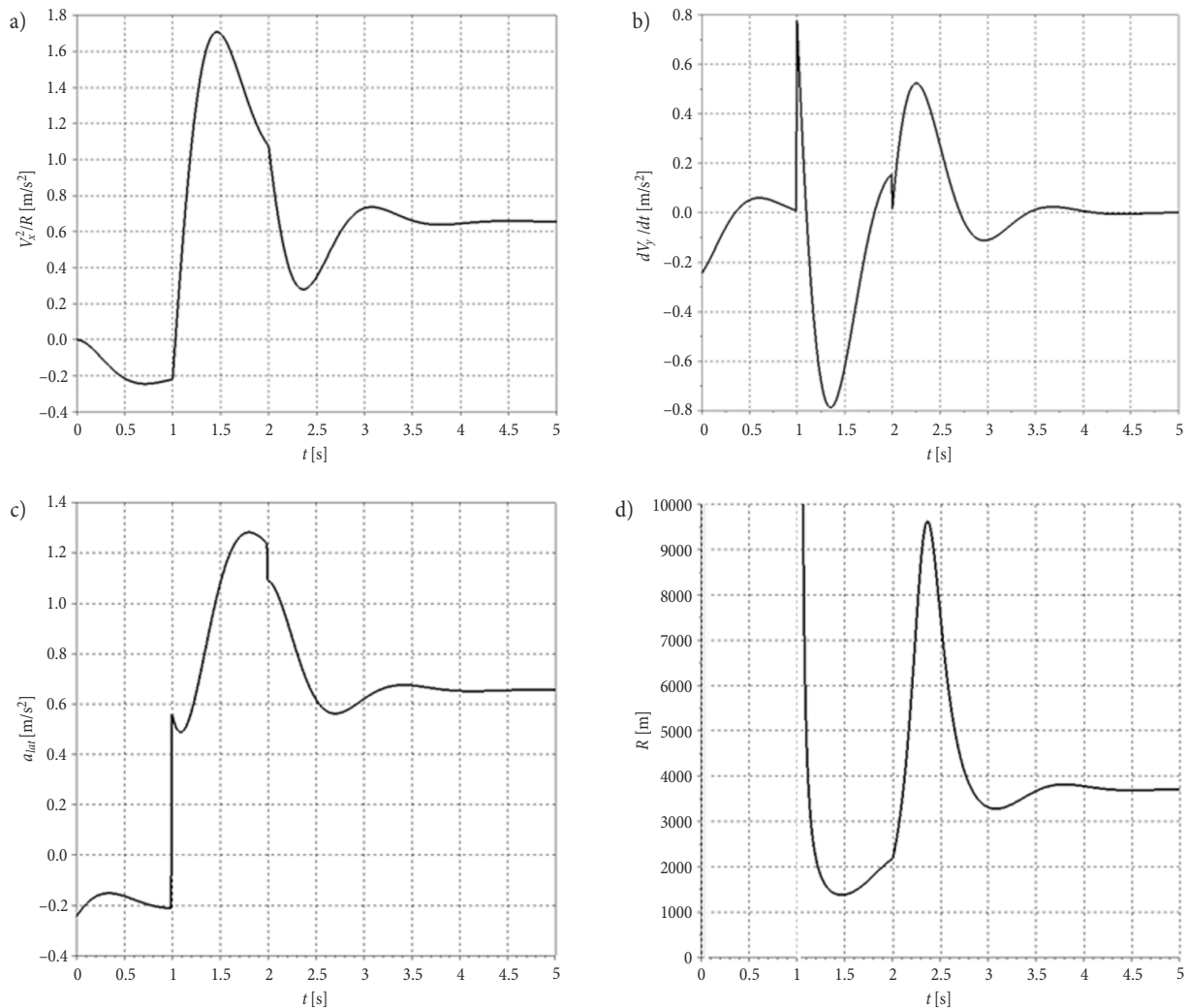


Fig. 5. Transient bicycle model results for scenario 1: a – lateral acceleration due to direction change of  $V_x$ ; b – lateral acceleration cause by tiredeformation; c – total lateral acceleration; d – path radius against time

However, for more intensive braking or for the case of a lower inflation pressure in the rear tires, the situation becomes drastically more dangerous. For example, decelerating more than  $3.5 \text{ m/s}^2$  with 25% underinflated rear tires leads to the so called oversteer vehicle behaviour. It means that the rear slip angle becomes greater than the front slip angle, so the circular movement increases the lateral acceleration and reduces the turning radius. It further increases the lateral acceleration and decreases the radius what can lead to the loss of vehicle stability and turning in the direction of the side force. The vehicle oversteer often results in an accident.

Tire cornering stiffness exponentially decreases with decreasing of inflation pressure. So, underinflated rear tires have to deform more for the same side friction demand. The combined effect of deceleration and underinflation of rear tires results in significant decrease of rear tires cornering stiffness what is included in bicycle model for scenario 3. The results of simulation for the third scenario, i.e. decelerating with  $3.5 \text{ m/s}^2$  and 25% underinflated rear tires, are presented in Fig. 6. Fig. 6c shows that the maximum value of total lateral acceleration is 15% greater than for the scenario without brak-

ing. It is a consequence of smaller path radii (Fig. 6d) due to higher deformation of the rear tires.

In order to better perceive the consequences on vehicle handling, trajectories in a global coordinate system for all scenarios are calculated using rotation matrix and presented in Fig. 7. The trajectories for both scenarios are almost the same until 1 second after the beginning of braking i.e. vehicle is assumed to be in the centre of lane driving parallel to lane marks.

For scenario 1 (no deceleration), the vehicle stays in the lane changing path radii because of tires deformation and steering.

In the case of scenario 2 (mild deceleration) there is a slow shift to the centre of the curve. 1 s (cca 45 m) after the separation of scenario 1 trajectory, vehicle position would be about 0.3 m closer to the centre of the curve (road curb).

For scenario 3 (intense decelerating and underinflated rear tires), there is a sudden drift to the centre of the curve and the vehicle hits the road curb in less than 1 s (45 m) after the beginning of trajectories separation, not giving the driver a good chance to take control of the vehicle.

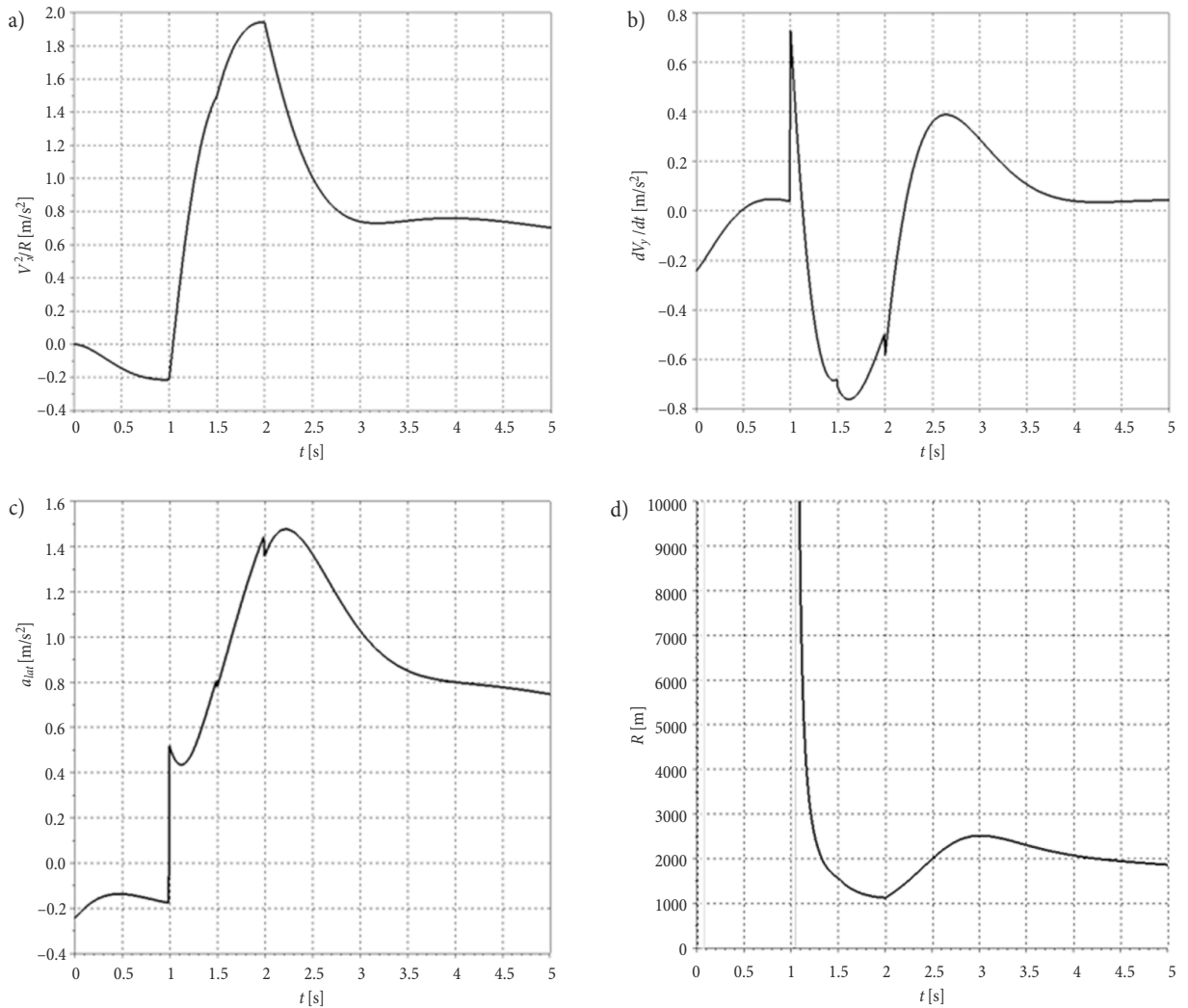


Fig. 6. Transient bicycle model results for scenario 3: a – lateral acceleration due to direction change of  $V_x$ ; b – lateral acceleration cause by tire deformation; c – total lateral acceleration; d – path radius against time

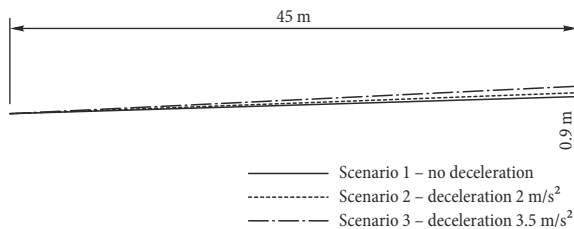


Fig. 7. Vehicles trajectories for 3 scenarios

The described situation with underinflated tires is very realistic and probable. According to a survey by Bridgestone Europe Group (2013), 78% of motorists in Europe drive with underinflated tires. Similarly for Canada and the US, a recent nationwide survey by the Rubber Manufacturers Association (Automotive Fleet 2010) in the US shows that 55% of vehicles have at least one underinflated tire and only one in six vehicles has all four properly inflated tires. National Automotive Sampling System Crashworthiness Data System (NASS-CDS) made a study where they found that about 36%

of passenger cars and about 40% of light trucks had at least one tire that was at least 20% below the placard pressure. About 26% of passenger cars and 29% of light trucks had at least one tire that was at least 25% below the placard pressure.

Therefore, the present study indicates that an unexpected situation caused by the road design or construction, which can result in an inappropriate manoeuvre could lead to a single-vehicle accident. The probability of accidents depends on the vehicle speed and condition as well as the driver’s experience and concentration. Less experienced and distracted drivers reduce the speed of their vehicle faster and more abruptly than non-distracted drivers, exhibiting excess braking comparatively (Haque 2015).

Preventive measures that are aimed specifically at reductions in single-vehicle accidents should be oriented towards the checking of road design consistency, mandatory introduction of specific in vehicle technology (a tire pressure monitoring system, electronic stability control) and driver awareness of traffic signalization.

## Conclusions

The paper tries to establish a procedure for detection and analysis of hazardous locations based on a real example, i.e., a few hundred meters long section on the motorway Zagreb–Split, where single-vehicle accidents happen regularly.

The analysed road section consists of two horizontal curves designed without spiral in transition and a negative superelevation. The test rides made at higher operating speeds showed that the application of a negative superelevation in the curves and the direct connection of the curves without spiral in a combination with a weak perception of the contact point between the curves, resulted in much smaller path radius than design one and jerk several times higher than the design value. Jerk could surprise a less concentrated driver and result in inappropriate manoeuvres, which could lead to the loss of vehicle stability. A vehicle dynamic model (bicycle or more complex 24 degree of freedom simulation model) can be used for analysis of the vehicle, tire and driver's characteristics, which could increase likelihood of single-vehicle accidents (speeding, underinflated tires, intense decelerating). The calculation of vehicle motion equations showed that braking can result in an increased slip angle on the rear wheels that can lead to the loss of vehicle stability.

The example stated above shows that, despite the fact that the road was designed in accordance with the design guidelines (in a term of alignment elements consistency) there is a possibility that some combination of alignment elements results in unexpected vehicle trajectory and high values of lateral acceleration change, especially for higher percentile operating speeds. These situations can lead to the single-vehicle accidents. In order to detect hazardous locations on roads before accidents happen it would be advisable to make a few test rides by experienced driver (with equipped vehicle) making common manoeuvres with higher percentile operating speed before the road is open to traffic.

The present research indicates that more attention has to be focused on the consistency of road elements, not only in a sense of speed consistency but also the acceleration change consistency, in order to eliminate unexpected situations, which can cause an inadequate driver reaction and accident.

The resulting knowledge about location and cause of inconsistency can greatly assist in determining the preventive measures to reduce the number of single-vehicle accidents, i.e. implementing traffic signals and devices in hazardous locations. Of course, a development of vehicle and tire technology and their mass implementation would significantly reduce the number of single-vehicle accidents.

The above stated considerations suggest that only an interdisciplinary approach (in vehicle and tire technology, road design, road construction, driver behaviour, etc.) could help to develop preventive approaches that are aimed specifically at reductions in single-vehicle accidents. In addition, great attention should be paid to

raising awareness of drivers to drive safely at speed adjusted to the road and weather conditions. Some of new in vehicle technology like tire pressure monitoring systems and electronic stability control are already mandatory (European Commission, 2008: Electronic Stability Control to be Standard on all Vehicles from 2014) in many countries, but there is a lot of room for improvement in a phase of checking the road design consistency after the construction of road and the use of traffic signalization aimed to hold driver awareness.

## References

- Automotive Fleet. 2010. *55% of Vehicles Have One Under-Inflated Tire*. Available from Internet: <http://www.automotive-fleet.com/news/story/2010/06/55-of-vehicles-have-one-under-inflated-tire.aspx>
- Baffet, G.; Charara, A.; Lechner, D. 2009. Estimation of vehicle sideslip, tire force and wheel cornering stiffness, *Control Engineering Practice* 17(11): 1255–1264. <http://doi.org/10.1016/j.conengprac.2009.05.005>
- Bridgestone Europe Group. 2013. *European Drivers Increasingly Negligent About the Maintenance of Their Tyres*. Available from Internet: <http://www.bridgestone.eu/corporate/press-releases/2013/04/european-drivers-increasingly-negligent-about-the-maintenance-of-their-tyres>
- Bundorf, R. 1967. The influence of vehicle design parameters on characteristic speed and understeer, *SAE Technical Paper 670078*. <http://doi.org/10.4271/670078>
- Cafiso, S.; Cava, G. 2009. Driving performance, alignment consistency, and road safety: real-world experiment, *Transportation Research Record: Journal of the Transportation Research Board* 2102: 1–8. <http://doi.org/10.3141/2102-01>
- Cafiso, S.; Cerni, G. 2012. New approach to defining continuous speed profile models for two-lane rural roads, *Transportation Research Record: Journal of the Transportation Research Board* 2309: 157–167. <http://doi.org/10.3141/2309-16>
- Cafiso, S.; Lamm, R.; La Cava, G. 2004. Fuzzy model for safety evaluation process of new and old roads, *Transportation Research Record: Journal of the Transportation Research Board* 1881: 54–62. <http://doi.org/10.3141/1881-07>
- Carlson, P. J. 1995. *Correlation of Ball Bank Indicator Readings and Lateral Acceleration*: PhD Thesis. Pennsylvania State University, US.
- Clark, S. K. (Ed.). 1971. *Mechanics of Pneumatic Tires*. National Bureau of Standards, Monograph 122. US Government Printing Office. Washington, DC.
- ERA-NET. 2012. *ERA-NET Road 2012: Safety at the Heart of Road Design*. Final Report of the ERA-NET programme.
- Fitzpatrick, K.; Miaou, S.; Brewer, M.; Carlson, P.; Wooldridge, M. 2005. Exploration of the relationships between operating speed and roadway features on tangent sections, *Journal of Transportation Engineering* 131(4): 261–269. [http://doi.org/10.1061/\(ASCE\)0733-947X\(2005\)131:4\(261\)](http://doi.org/10.1061/(ASCE)0733-947X(2005)131:4(261))
- Gibreel, G.; Easa, S.; El-Dimeery, I. 2001. Prediction of operating speed on three-dimensional highway alignments, *Journal of Transportation Engineering* 127(1): 21–30. [http://doi.org/10.1061/\(ASCE\)0733-947X\(2001\)127:1\(21\)](http://doi.org/10.1061/(ASCE)0733-947X(2001)127:1(21))
- Gibreel, G.; Easa, S.; Hassan, Y.; El-Dimeery, I. 1999. State of the art of highway geometric design consistency, *Journal of Transportation Engineering* 125(4): 305–313. [http://doi.org/10.1061/\(ASCE\)0733-947X\(1999\)125:4\(305\)](http://doi.org/10.1061/(ASCE)0733-947X(1999)125:4(305))

- Haque, M. M. 2015. The impact of mobile phone distraction on the braking behaviour of young drivers: a hazard-based duration model, *Transportation Research Part C: Emerging Technologies* 50: 13–27. <http://doi.org/10.1016/j.trc.2014.07.011>
- Hassan, Y. 2004. Highway design consistency: refining the state of knowledge and practice, *Transportation Research Record: Journal of the Transportation Research Board* 1881: 63–71. <http://doi.org/10.3141/1881-08>
- Hassan, Y.; Sayed, T.; Taberner, V. 2001. Establishing practical approach for design consistency evaluation, *Journal of Transportation Engineering* 127(4): 295–302. [http://doi.org/10.1061/\(ASCE\)0733-947X\(2001\)127:4\(295\)](http://doi.org/10.1061/(ASCE)0733-947X(2001)127:4(295))
- Himes, S.; Donnell, E.; Porter, R. 2011. New insights on evaluations of design consistency for two-lane highways, *Transportation Research Record: Journal of the Transportation Research Board* 2262: 31–41. <http://doi.org/10.3141/2262-04>
- Hrvatske Autoceste. 2015. *Hrvatske autoceste d.o.o.* Available from Internet: <http://hac.hr> (in Croatian).
- Jessen, D.; Schurr, K.; McCoy, P.; Pesti, G.; Huff, R. 2001. Operating speed prediction on crest vertical curves of rural two-lane highways in Nebraska, *Transportation Research Record: Journal of the Transportation Research Board* 1751: 67–75. <http://doi.org/10.3141/1751-08>
- Krammes, R. A.; Rao, K. S.; Oh, H. 1995. Highway Geometric Design Consistency Evaluation Software, *Transportation Research Record: Journal of the Transportation Research Board* 1500: 19–24.
- Lamm, R.; Psarianos, B.; Choueiri, E. M.; Soilemezoglou, G. 1995. A practical safety approach to highway geometric design international case studies: Germany, Greece, Lebanon, and the United States, in *International Symposium on Highway Geometric Design Practices*, 30 August – 1 September 1995, Boston, Massachusetts, US, 9-1–9-14.
- Marchionna, A.; Perco, P. 2008. Operating speed-profile prediction model for two-lane rural roads in the Italian context, *Advances in Transportation Studies* 14: 57–68.
- Mattar-Habib, C.; Polus, A.; Farah, H. 2008. Further evaluation of the relationship between enhanced consistency model and safety of two-lane rural roads in Israel and Germany, *European Journal of Transport and Infrastructure Research* 8(4): 320–332.
- Medina, A. F.; Tarko, A. P. 2005. Speed factors on two-lane rural highways in free-flow conditions, *Transportation Research Record: Journal of the Transportation Research Board* 1912: 39–46. <http://doi.org/10.3141/1912-05>
- Moyer, R. A.; Berry, D. S. 1940. Marking highway curves with safe speed indications, *Highway Research Board Proceedings* 20: 399–428.
- MPPV. 2001. *Pravilnik o osnovnim uvjetima kojima javne ceste izvan naselja i njihovi elementi moraju udovoljavati sa stajališta sigurnosti prometa*. NN 110/01. Ministarstvo pomorstva, prometa i veza (MPPV). Available from Internet: [http://narodne-novine.nn.hr/clanci/sluzbeni/2001\\_12\\_110\\_1829.html](http://narodne-novine.nn.hr/clanci/sluzbeni/2001_12_110_1829.html) (in Croatian).
- NHTSA. 2001. *Tire Pressure Special Study*. US Department of Transportation, National Highway Traffic Safety Administration (NHTSA), Washington, DC.
- Ng, J. C. W.; Sayed, T. 2004. Effect of geometric design consistency on road safety, *Canadian Journal of Civil Engineering* 31(2): 218–227. <http://doi.org/10.1139/l03-090>
- Nordeen, D.; Cortese, A. D. 1964. Force and moment characteristics of rolling tires, *SAE Technical Paper* 640028. <http://doi.org/10.4271/640028>
- Ottesen, J.; Krammes, R. 2000. Speed-profile model for a design-consistency evaluation procedure in the United States, *Transportation Research Record: Journal of the Transportation Research Board* 1701: 76–85. <http://doi.org/10.3141/1701-10>
- Park, Y.-J.; Saccomanno, F. F. 2006. Evaluating speed consistency between successive elements of a two-lane rural highway, *Transportation Research Part A: Policy and Practice* 40(5): 375–385. <http://doi.org/10.1016/j.tra.2005.08.003>
- Perco, P. 2008. Influence of the general character of horizontal alignment on operating speed of two-lane rural roads, *Transportation Research Record: Journal of the Transportation Research Board* 2075: 16–23. <http://doi.org/10.3141/2075-03>
- SAE International. 2008. *Vehicle Dynamics Terminology*. SAE J670 Standard. Society of Automotive Engineers (SAE). 73 p.
- Sandberg, U.; Ejsmont, J. A. 2002. *Tyre/Road Noise Reference Book*. Informex. 640 p.
- Schurr, K.; McCoy, P.; Pesti, G.; Huff, R. 2002. Relationship of design, operating, and posted speeds on horizontal curves of rural two-lane highways in Nebraska, *Transportation Research Record: Journal of the Transportation Research Board* 1796: 60–71. <http://doi.org/10.3141/1796-07>
- TRB. 2011. *Modeling Operating Speed: Synthesis Report*. Transportation Research Circular Number E-C151. Transportation Research Board (TRB), Washington, DC. 136 p. Available from Internet: <http://onlinepubs.trb.org/onlinepubs/circulars/ec151.pdf>
- Wang, Y.; Xu, G.; Bai, H. 2013. Operating speed based alignment consistency evaluation using driving simulator: case studies from Taigan freeway in Jiangxi, China, *Promet – Traffic & Transportation* 25(1): 23–31. <http://doi.org/10.7307/ptt.v25i1.1244>
- Wong, J. Y. 2008. *Theory of Ground Vehicles*. 4th edition. Wiley. 592 p.